Modelling the Ruin of Forests under Climate Hazards

Pascal Yiou[1] and Nicolas Viovy[1]

[1]Laboratoire des Sciences du Climat et de l'Environnement, UMR 8212 CEA-CNRS-UVSQ, IPSL & U Paris-Saclay, 91191 Gif-sur-Yvette Cedex, France

Correspondence: P. Yiou (pascal.yiou@lsce.ipsl.fr)

Abstract. Estimating the risk of collapse of forests due to extreme climate events is one of the challenges of adaptation to climate change. We adapt a concept from ruin theory, which is widespread in econometrics or the insurance industry, to design a growth/ruin model for trees, under climate hazards that can jeopardize their growth. This model is an elaboration of a classical Cramer-Lundberg ruin model that is used in the insurance industry. The model accounts for the interactions between

5 physiological parameters of trees and the occurrence of climate hazards. The physiological parameters describe interannual growth rates and how trees react to hazards. The hazard parameters describe the probability distributions of occurrence and intensity of climate events. We focus on a drought/heatwave hazard. The goal of the paper is to determine the dependence of ruin and average growth probability distributions as a function of physiological and hazard parameters. From extensive Monte Carlo experiments, we show the existence of a threshold on the frequency of hazards beyond which forest ruin becomes certain

10 in a centennial horizon. We also detect a small effect of strategies to cope with hazards. This paper is a proof-of-concept to quantify collapse (of forests) under climate change.

1 Introduction

If one adopts the (debatable) dogma that ecosystems provide services to society, one must also accept that such services could

15 disappear under natural or human made hazards. In many instances, such ecosystems are considered as "investments" that "investors" want to fructify some time later. A challenge is to estimate the risks associated to such investments.

There has been ample literature on *tipping points* of the climate system, i.e. climate thresholds beyond which ecosystems change behavior (Lenton et al., 2008; Levermann et al., 2012). Most of those papers are rather qualitative in that they do not give probabilities of "tipping point" nor provide a timing for such changes. A consequence is that policymakers make little use

20 of those studies, because risks are rarely estimated in precise ways.

A body of literature on so-called *collapsology* has emerged in the past few years (Diamond, 2005). Those studies describe mechanisms that would make the key institutions of society collapse due to an accumulation of big or small events. Again, those considerations are generally qualitative as to "when" and "how intense", as they address very general issues and no mechanistic model of a collapsing system is analyzed.

25 Most of those studies are useful to raise awareness on the dangers of climate change, but are rarely included in decision chains. On the other hand, there have been many papers in the econometrics literature that describe ruin models for insurance and finance since the seminal work of Lundberg (1903). A mathematical and statistical artillery (Asmussen and Albrecher, 2010) has helped determining the optimal parameters of such models, so that insurers or investors limit the risk of losing their investment and maximize their gain. To the best of our knowledge, this literature has never been transposed to environmental

30 sciences, although it provides all the tools for decision making, which are used daily in insurance and finance.

The goal of this paper is to obtain quantitative parameters that describe the ruin of ecosystems. We chose to focus on forestry, for which mechanistic growth models can be devised (e.g. Han and Singh, 2020) and observations are available (e.g. Choat et al., 2012). Tree growth is affected by climate variations in various ways. Heatwaves and droughts can alter (and lower) tree reserves and capability for growth on next years, which affects their growth and can increase their chance of mortality (von

35 Buttlar et al., 2017; Sippel et al., 2018). The recent accumulation of drought/heat stress to forests might lower their resilience to future extreme events (e.g. Wigneron et al., 2020; Flach et al., 2018; Bastos et al., 2020). Several studies have investigated the processes leading to tree mortality from observations (Adams et al., 2009; Bigler et al., 2007; Bréda and Badeau, 2008; Villalba and Veblen, 1998; Matusick et al., 2018).

A parallel between insurance system and trees can be done. As opposed to annual plants, trees are adapted to live for a long

40 time and then should be able to avoid death related to damage due to bad climate conditions during a year. Those damages can be related to a reduced productivity and in the worst cases to a destruction of a part of the trees (related for instance to xylem embolism that kills the branches). For this purpose they contain a large amount of carbohydrate and a structure (branches) that allow to build rapidly a large surface of leaves (potential productivity been related to this foliage area)) on the next year and protect from pathogen disease even if the productivity of the previous year was reduced or because of events like defoliation

45 (e.g insects). Hence a part of annual productivity is devoted to accumulate carbohydrate reserves (larger than what is necessary for next year initiation of the vegetative cycle) and ensure a structure that allows to support leaves. This can be compared to an insurance system when each year, a part of the productivity is "payed" to the insurance (i.e carbohydrate reserves) but in return can be mobilized in case of damage. Then "ruin" occurs when trees die because of carbon starvation as level of carbohydrate reserves and productivity is not sufficient to maintain respiration cost.

50 Our study investigates the probability of "ruin" of a population of trees that are subjected to heat and drought stress. We introduce a simple tree growth model based on the Cramer-Lundberg ruin model for insurances (Embrechts et al., 1997). We investigate its properties in order to evaluate the occurrence of ruin (i.e. disappearance of trees) within a fixed horizon, due to the impacts of extreme events, under various climate change scenarios. This approach is meant to tackle quantitatively the issues of tipping points or collapse for a specific field (forestry), although this could be extended to other domains. By *quantitative*, we

55 mean that we determine the probability distributions of key ruin parameters (e.g., time of ruin and average capital). Unlike the Cramer-Lundberg ruin model, our tree model cannot be solved explicitly and we will resort to extensive numerical simulations, as a standard sample for the insurance industry has to contain more than 10^4 members for proper probability estimates.

In section 2 we introduce a growth/ruin model for trees based on a Cramer-Lundberg ruin model, and discuss the interpretation of its parameters. In section 3 we detail the meteorological data that are used to construct a hazard function. Section 4

explains the experimental protocol for the analyses. The results and interpretations are developed in section 5. An Appendix is
devoted to the development of a drought index based on precipitation and temperature.

2 Methods

2.1 Cramer-Lundberg ruin model

This section introduces the key concepts to ruin models. The insurance industry uses such statistical models to determine the
premium prices, in order to achieve a balance between competing companies and minimize the risk of ruin (i.e. when the
capital vanishes). Those statistical models are based on the simple Cramer-Lundberg model, which can be formulated as:

$$R(t) = R_0 + pt - S(t), \tag{1}$$

where $R(t)$ is the capital at time t, $R_0 > 0$ is the initial capital, $p > 0$ is the premium rate that is collected every year t, and
$S(t) \geq 0$ represents the (random) losses to hazards that occur up to time t. The only random part of the model in Eq. (1) stems
from the loss $S(t)$. A ruin is declared and the process is stopped when $R(t) \leq 0$.

One can be interested in the behavior of the system before a finite horizon $T > 0$, e.g. a few decades. We define the ruin
probability Ψ before horizon T by:

$$\Psi(R_0, p, T) = \Pr\left(R(t) \leq 0, \text{ for some } T \geq t > 0\right) \tag{2}$$

and the ruin time $\tau(R_0, p, T)$:

$$\tau(R_0, p, T) = \inf\{t > 0, R(t) \leq 0\}. \tag{3}$$

Since $S(t)$ is a random process, we are interested in $E(\tau)$, the expected value of τ with respect to the random variable $S(t)$.
If ruin never occurs during simulations of R, then $E(\tau) = \infty$. Actors in insurance companies try to estimate the smallest p
rate from expert knowledge on the probability distribution of $S(t)$ in order to avoid ruin, which would give them a lead in the
competition against more greedy companies (which are subject to the same hazards $S(t)$).

In several instances, there is no acceptable value for p to prevent from ruin, i.e. the probability distribution of the expected
value of τ can be lower than the value T (say, with some low probability). This is why insurance companies resort to re-
insurance to avoid bankruptcy after unexpectedly large losses $S(t)$.

The losses $S(t)$ are generally represented as a *random sum* of random variables:

$$S(t) = \sum_{k=1}^{N(t)} X_k, \tag{4}$$

where $N(t)$ is a Poisson random variable that accounts for the number of hazards occurring up to time t, and X_k are random
variables that account for the cost of each hazard. The probability distribution of X_k can be modeled by an extreme value

law, like a generalized Pareto distribution (GPD) (Coles, 2001; Embrechts et al., 1997), when a hazard variable exceeds a high threshold u. The GPD describes the probability distribution of a random variable X when its value exceeds a threshold u:

$$\Pr\{X > x | X > u\} = \left[1 + \xi\left(\frac{x - \mu}{\sigma}\right)\right]^{-1/\xi}, \tag{5}$$

90 where $\sigma > 0$ is a scale parameter and ξ is a shape parameter that states how fast extremes grow. The parameters of the Poisson distribution for $N(t)$ and the GPD distribution are estimated from prior information, e.g. observations or expert knowledge.

There is ample statistical literature in finance on the relation between τ and the probability distribution of S (Embrechts et al., 1997; Asmussen and Albrecher, 2010). In practice, estimates of $E(\tau)$ or an optimal p can be obtained by simulating the model of Eq. (1) and estimating empirical probability distributions.

95 The notion of finite horizon T is useful when considering that an investment (in the insurance sector) is made for a finite time. We will be interested in generating many finite sequences of $S(t)$, corresponding to a sample of all possible T-long trajectories.

2.2 A ruin model for trees

The goal of this sub-section is to adapt the Cramer-Lundberg model in Eq. (1) to formulate a simple tree growth model that
100 explicitly takes into account a climate hazard $S(t)$.

Here $R(t)$ is the non-structural carbohydrates (hereafter called reserves) that allows growth of tree at the beginning of vegetative period. We assume that trees spend a fraction of their resources to grow roots and leaves, depending on their previous state. We also assume that tree resources are bounded by an optimal value $R_{\max}$. It has been observed legacy effects of drought hazard on the trees growth the year after it. (cite Handeregg). which depend on the tree species. Because of this
105 decreased NPP, we assume that it will also affect allocation to carbohydrate reserves. Hence, the yearly net primary production (NPP) allocated to reserves $p(t)$ depends on the climate hazard that occurred during the previous year $S(t-1)$:

$$p(t) = p_0 - BS(t-1), \tag{6}$$

where p_0 is the optimum average yearly NPP of a population of trees allocated to reserve, and $B \geq 0$ is a memory factor of the damage function. We hence introduce a new growth/ruin model for trees:

110 $$R(t) = \min\left[(1 - b)R(t-1) + p(t) - S(t), R_{\max}\right], \tag{7}$$

where $b \geq 0$ is the fraction of previous resources (at time $t-1$) devoted to growth. In this model, the parameters b, B and $R_{\max}$ are called *physiological* as they describe tree growth.

In this paper, we suppose that the type of hazards that can affect tree growth (or survival) are summer droughts (Allen et al., 2010; Choat et al., 2012; DeSoto et al., 2020). In Europe, major summer heatwaves are often concomitant with droughts.
115 This combination of climate factors creates a stress to trees, which lowers their NPP and can destroy branches and leaves and impacts their growth and reserve. Other types of hazards could also be considered (storms, pests, etc.). Hence we consider drought/heatwave (HW) hazards. We declare that ruin is reached when $R(t) = 0$.

The hazards do not necessarily occur every year: they arrive at times t that follow an exponential distribution with parameter Λ. Thus the inter-arrival times follow a Poisson distribution with a mean value of $\theta = 1/\Lambda$ (the average return time of hazards).

120 This description is rather generic in standard queuing models (Feller, 1950). When climate hazards occur (at random times), $S(t)$ is written as:

$$S(t) = A_h \sum_{k=1}^{N(t)} X_k. \tag{8}$$

A_h is a normalizing constant that translates the climate hazard conveyed by X_k into damage to $R(t)$. $N(t)$ is the number of hazards (e.g. the number of very hot/dry days) during year t and follows a Poisson distribution with parameter λ. X_k are

125 climate variables like a drought index for heatwaves or wind speed for storms during hazards, and follow generalized Pareto distributions (GPD), with scale parameter σ and shape parameter ξ. The GPD describes the probability distribution of X_k when it exceeds a high threshold u (Coles, 2001). The parameter of the GPD (σ and ξ) and the occurrence of events (λ and Λ) are called the *hazard* parameters.

When no hazard occurs, $S(t) = 0$. If $b = 0$ (no use of reserves for growth), $B = 0$ (no memory of previous hazard) and

130 $N_h(t) = 1$ (only one hazard at a time at most), then the model in Eq. (7) simplifies to the Cramer-Lundberg ruin model (Eq. (1)), in which $N(t)$ follows a Poisson distribution of parameter Λ. If hazards never occur (i.e. $S = 0$ at all times), then $R(t)$ converges to $(1 - b)R_{\max}$.

The parameters of the Poisson distributions for $N_h(t)$ and the Pareto distributions for X_k can be estimated experimentally from meteorological observations or climate model simulations. The growth parameters p, b and $R_{\max}$ in Eq. (7) can be

135 obtained from tree physiology databases (Allen et al., 2010; Cailleret et al., 2017) and should be adapted to tree species.

The difficult part is to estimate scales for the values of A_h and B. It has been observed that tree species can have differing strategies to face heat and drought stress (Adams et al., 2009; Teuling et al., 2010): some tree species grow in spite of the hazard during year t. this can be achieved by maintaining stomatal aperture to maintain photosynthesis (anisohydric strategy) increasing the risk of embolism (Mitchell et al., 2013) or changing allocation to maintain growth of branches and root at

140 expense of carbohydrate reserves (van der Molen et al., 2011). In both cases, these trees "pay" the next year, even if there is no hazard because maintaining the plant growth will be at expense of foliage surface and plant protection on next year (van der Molen et al., 2011). Those are trees with interannual memory. Conversely other tree species stop growing during hazards (by stomatal closure to avoid embolism (isohydric strategy) or maintain allocation to reserve at the expense of other pools) at t, For these trees, the impact on growth on the year of hazard is important, but this hazard has few impacts on next year. Those

145 are trees without interannual memory. It is possible to represent the different strategies in the model through the parameter B. Hence the first strategy (i.e maintaining growth, interannual memory) can be represented by high value of B in Eq. (6). Conversely the second strategy (i.e conservative, no memory) can be represented by B close to 0 in Eq. (6). We will investigate the sensitivity of the ruin probabilities to those tree strategies. Therefore, to simplify things, making a parallel with an insurance system: if $B = 0$, trees pay "cash" on their reserve ($S(t)$ then will be large); if $B > 0$ they allow for a "credit" to the next year

150 ($S(t)$ is reduced but will impact possibility to use reserve on next year). Mitchell et al. (2013) notice that in reality, there is a continuum between the two strategies which can be represented by the value given by B. The values of B are chosen so that

the average value of damages (i.e., the expected value of $(1+B)S(t)$) is a constant. This constant gives the scale of the impact parameter A_h.

In this paper, the values of A_h and B are arbitrarily chosen to scale with an expected behavior of trees. The range of those
155   parameters could be estimated from in situ observations or expert knowledge.

2.3 Sample trajectories

The time variations of this model are illustrated with parameters of tree growth $p = 5$, $b = 0.05$, $A_h = 0.6$, $R_{\max} = 100$. The hazard parameters are $\sigma = 0.1$, $\xi = -0.2$ and threshold $u = 1$ (from the GPD distribution), and $\lambda = 10$ days and $\Lambda = 5$ years for the hazard arrivals. The model was run with memory parameter values of $B = 0$ ("cash") and $B = 1.5$ ("credit"). We simulated
160   10^4 trajectories with those parameters. For each ensemble, we computed the average of the reserve function $R(t)$. We selected four trajectories with the 95th, median and 5th quantiles of the average reserve function, one of the trajectories with a ruin.

Figure 1ab shows the time series of the damage $S(t)$ and the reserve $R(t)$ functions for three key trajectories, when $B = 0$. As the shape parameter ξ is negative, the damage values $S(t)$ do not yield a large variability. The reserve averages for the 5th, 95th and median trajectories are respectively 42, 59 and 69 reserve units.
165   Figure 1c,d shows the time series of the damage $S(t)$ and the reserve $R(t)$ functions for four key trajectories, when $B = 1.5$. The damage function yields the same statistical properties but the scaling is different so that the integrated damages are similar in both cases: the hazard is scaled so that the damage at year t is distributed over t and $t + 1$. On this sample of simulations, the reserve averages for the 5th, 95th quantiles and median trajectories are respectively 42, 46 and 69 reserve units. Hence, the reserve is generally lower, although the ruin time could occur later. The time variability of $R(t)$ is smoother as $B = 1.5$
170   introduces an interannual memory of hazards. This explains the long-time variability of the median trajectory, compared to Figure 1ab.

Those two samples of parameters illustrate that the coping strategies do influence the behavior of the modeled trees. Ruin can occur faster for $B = 0$ (paying "cash"), although the median of the reserve is higher. The rest of the paper is devoted to quantify those differences.
175   A lot of data have been collected from death trees and from surrounding trees still alive to evaluate how death trees behave years before they die (e.g Villalba et al. (1998), Bréda and Badeau (2008)). Hence difference of tree rings width between dead and living tree (that allow to remove the influence of annual climate condition) can be considered as a good proxy of tree reserves. Cailleret et al. (2017), for instance made a synthesis of existing data and investigated tree ring growth years before tree death, under various climate hazards. It is interesting to notice that there is a good agreement between our simulated
180   evolution of reserves in case of ruin (Figure 1 b,d) and observed evolution of tree ring width before tree dying. In particular Cailleret et al. (2017) show that in the majority of the cases, there is an observed relative decrease of growth (compared to healthy trees) between twenty to fifty years before death which is coherent with our simulations.
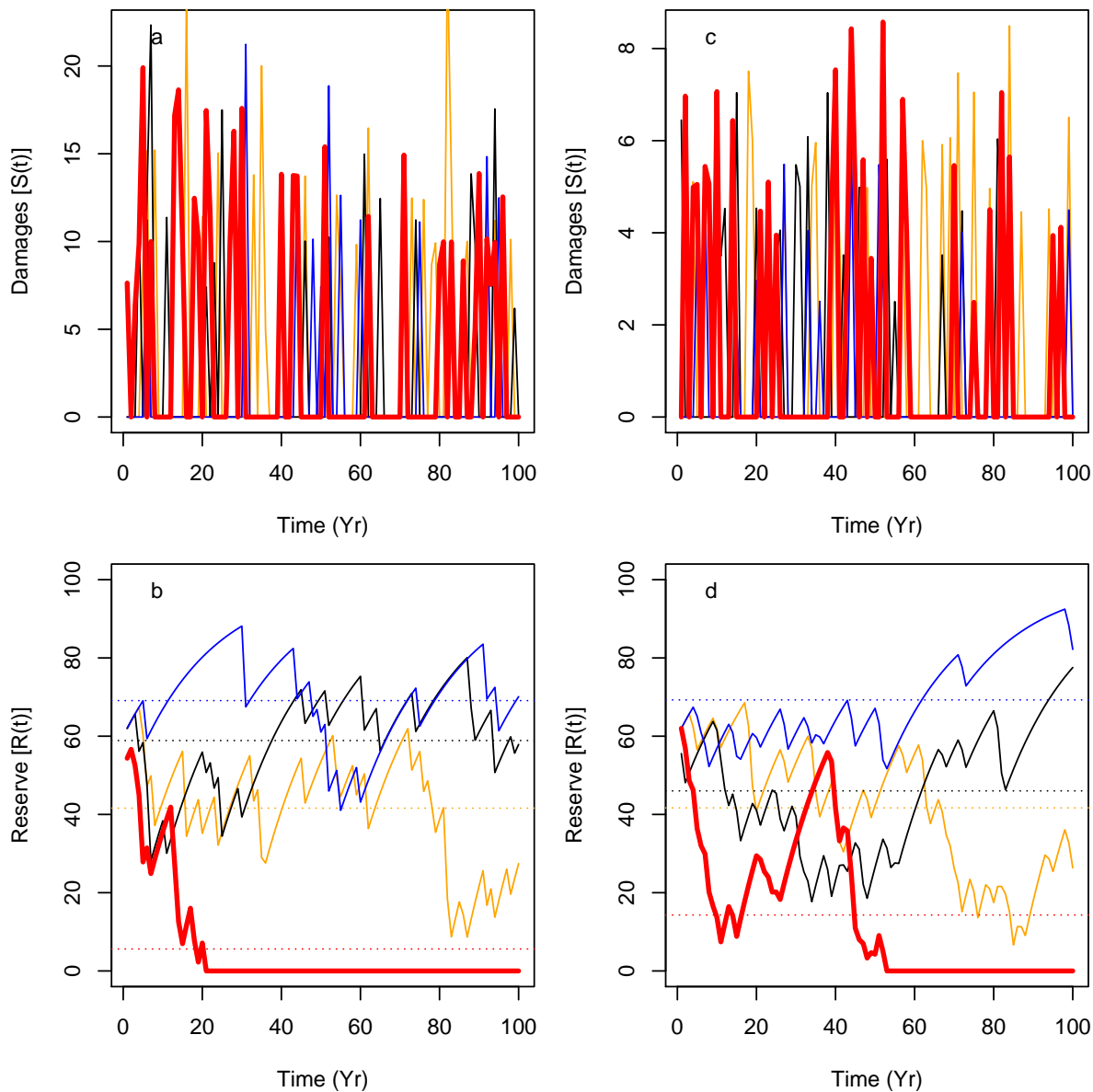
Figure 1. Sample of four time series of simulations of $S(t)$ (upper panels) and $R(t)$ (lower panels) for $B = 0$ ("cash": panels a and b) and $B = 1.5$ ("credit": panels c and d). The blue lines are the trajectories of S and R that achieves the median of the average of R (among 10^4 simulations). The black lines are for the trajectories of the 95th quantile of R. The orange lines are for the 5th quantile trajectories of R. The red lines is for trajectories with ruin. The horizontal dotted lines indicate the mean $R(t)$ values of the trajectories.

3   Data

The goal of this section is to provide climate constraints on the parameters of the hazard function $S(t)$.

3.1 Observations

Meteorological data were taken from the European Climate and Data (ECA&D) database (Haylock et al., 2008). We used daily maximum temperature (TX) and daily precipitation (RR) from Berlin, De Bilt, Orly, Toulouse and Madrid stations. This choice was motivated to cover a rather large range of European latitudes and longitudes over western Europe. We considered data from 1948 to 2019 (> 70 years of daily data). Those datasets yield less than 10% of missing observations.

3.2 Drought/heatwave damage index

We consider the drought/heatwave index I_{YV} defined in the Appendix A, based on precipitation frequency and temperature from the ECA&D database. This index is computed over five ECA&D stations (Berlin, De Bilt, Orly, Toulouse and Madrid).

From the Spring-Summer variations of this index, we determine the Generalized Pareto Distribution parameters of the daily I_{YV} indice, when the (daily) values exceed the 95th quantile. As the daily values are temporally correlated (by construction, as the indice is a running sum), we consider the maxima of clusters above the 90th quantile and determine the number of days that exceed the 95th quantile threshold. This procedure is advocated in the textbook of Coles (2001).

The values and standard errors of the GPD parameters (scale and shape) are shown in figure 2.

We considered the range of parameters obtained from the 5 stations and their uncertainties, and took a conservative envelope of those parameters and their lower and upper uncertainties. From those ranges of parameters, we can simulate Generalized Pareto distributions for the damage function in the model of Eq. (8).

4 Experimental design

The physiological parameter in Eq. (7) are fixed to $b = 0.05$, $p = 5$ and $R_{\max} = 100$. We simulate $N = 10^6$ trajectories of $R(t)$ of 100 years, with an initial condition of $R(0) = 60$.

For each trajectory, the parameters of the damage function $S(t)$ are randomly sampled with a uniform distribution with a range that is estimated from the heat/drought stress indice I_{YV} (in Sec. 3). The bounds of the uniform distributions are given in table 1, which are conservative bounds of Figure 2.

From those ensembles of simulations trajectories we determine the average of reserve $R(t)$ before ruin $\langle R \rangle$, and the time of ruin T_{ruin} (if it ever occurs). By construction of the model, $R(t)$ evolves between 0 and 80 (the optimal reserve) and T_{ruin} is between 1 (immediate ruin) and 100 (no ruin within 100 year simulations).

The large number of trajectories (10^6) helps investigate the dependence of $\langle R \rangle$ and T_{ruin} on the parameters of S, namely σ, ξ, λ and Λ (see table 1).

5 Results

The dependence of the ruin time on the four damage parameters is shown in Figure 3 when $B = 0$. Each boxplot depicts the probability distribution of ruin times for a given value of a parameter, and a random combination of other parameters.
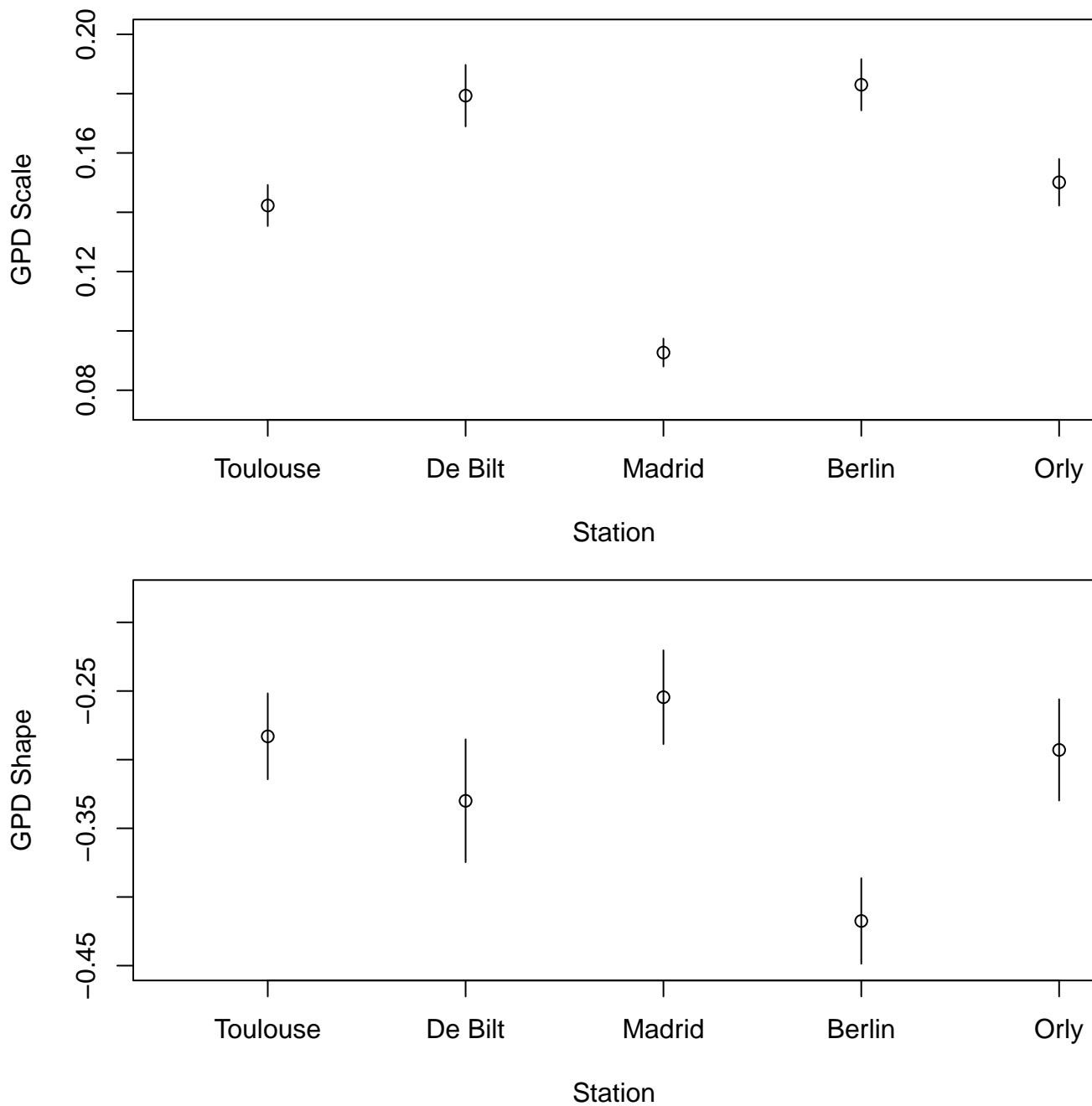
Figure 2. Distribution of scale (upper panel) and shape (lower panel) parameters of the I_{YV} indice for Berlin, De Bilt, Orly, Toulouse and Madrid. The vertical bars represent the 95% confidence intervals of the estimates.

Table 1. Range of values of parameters for the damage function $S(t)$. The bounds are conservative values read from Figure 2.

Parameter	Interpretation	range
u	GPD threshold	$[1; 5]$
σ	GPD Scale	$[0.08; 0.2]$
ξ	GPD shape	$[-0.45; -0.2]$
λ	Nb. dry days	$[2; 30]$
Λ	Return period of HW (years)	$[2; 15]$

215 Figure 3 highlights the fact that the system can shift from a "no ruin" state to a probable ruin in a century, with rather small parameter changes of the frequency of hot days (either the frequency of dry/hot summers, or the number of dry/hot days during a hot summer). The dependence on the scale parameter σ and the shape parameter ξ is rather weak (Figure 3cd). The prescribed range of variations of those GPD parameters is small in absolute values. The GPD threshold u has an important impact of the ruin time, as the probability distribution of ruin times shift from a median on 100 years to a median value of 70 years within a

220 6% change of the threshold u (Figure 3e).

From this experiment, we find that a "no ruin/ruin" bifurcation occurs when a return period threshold of 8 years is crossed (Figure 3a) is crossed. If we focus on western Europe, extreme summer heatwaves and droughts occurred in 2003, 2006, 2018 and 2019. This might imply that European forests with trees that yield those physiological parameters are close a threshold of ruin.

225 The threshold on the number of hot days per summer is 14 days (Figure 3b). This parameter controls the magnitude of the random sum in $S(t)$, because the daily hazards X_k yield a bounded tail ($\xi < 0$). This means that if the length of heatwaves can exceed 14 days, tree ruin becomes significantly likely before the end of the 100 years.

The probability distribution of the average reserve before ruin $\langle R \rangle$ is shown in Figure 4 for trees with $B = 0$. This figure highlights that $\langle R \rangle$ weakly depends on the GPD parameters of the damage function (Figure 4cd). The average reserve strongly

230 depends on the return period of heatwaves and the number of hot days during heatwaves and the GPD threshold u (Figure 4abe).

Figure 4a shows that when damages (due to droughts/heatwaves) occur too often (low return periods of events), then the trees do not have enough time to build enough reserves to face the next extremes.

The behavior of tree growth when $B = 1.5$ ("credit") is very similar to the one with $B = 0$ ("cash") as the differences are

235 relatively small (not shown): the median reserve for the "cash" simulations appear slightly higher than the "credit" simulations.

In a second set of experiments, we maintain the scale and shape parameters constant: $\sigma = 0.1$ and $\xi = -0.3$. The other hazard parameters are randomly sampled within the range as indicated in Table 1. As observed in Figure 3ab, a transition from a median ruin time of 100 years (i.e. no or unlikely ruin) to a ruin time $\tau < 100$ years appears for return times of events Λ near 8 years, duration of events λ of 14 days or GPD threshold u of 2.75. Therefore, we focus on the probability distributions of

240 ruin times and reserve near those thresholds, for the "cash" ($B = 0$) and "credit" ($B = 1.5$) simulations.
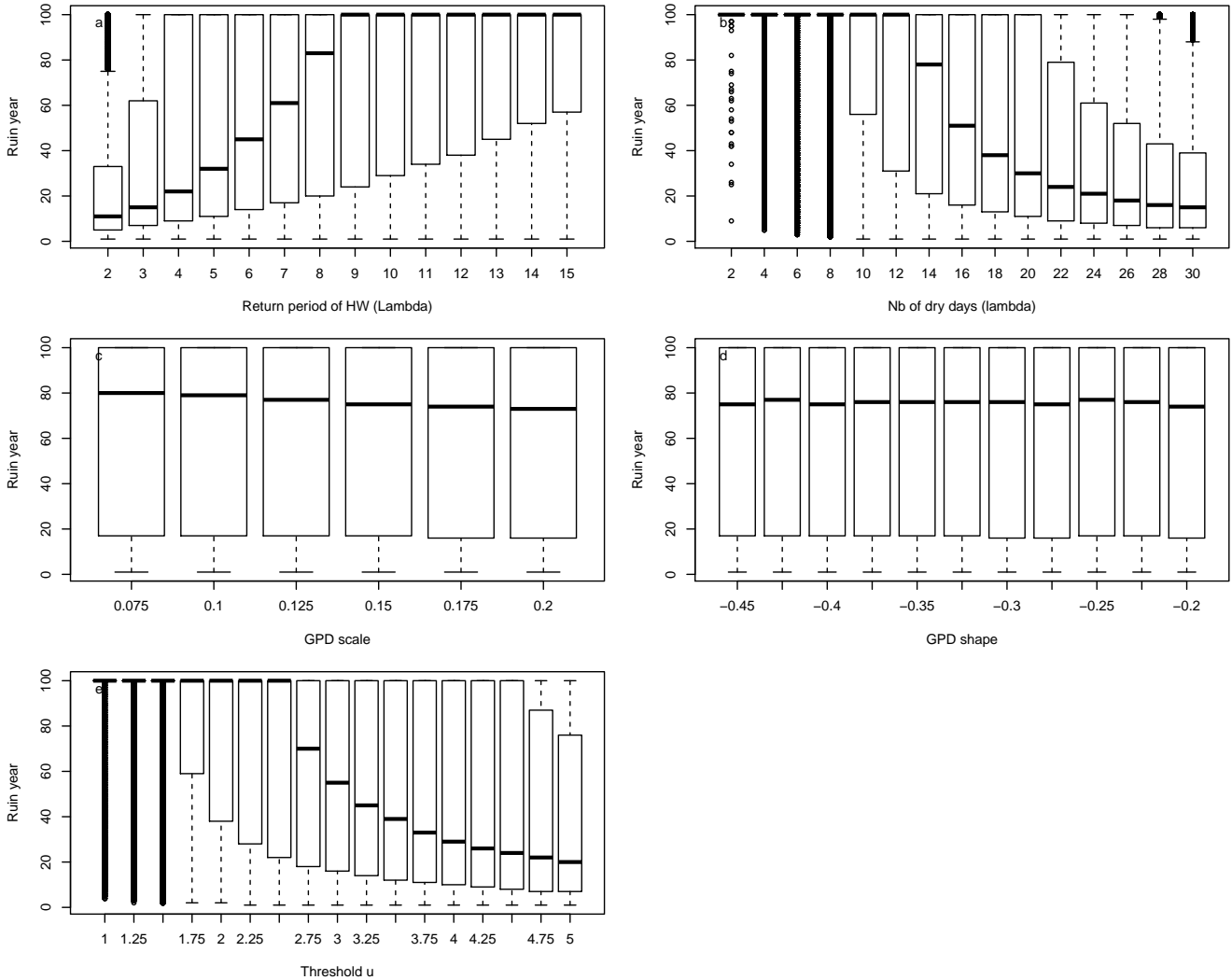
Figure 3. Dependence of probability distributions of ruin year τ as a function of heatwave (HW) return periods Λ (a), number of hot days during summers λ (b), GPD fit scale μ (c) and GPD fit shape ξ (d), and threshold u above which damage $S(t)$ is triggered (e). For each value of the control variable, a boxplot is given. The horizontal thick bar of boxplots represents the median ($q50$) of the distribution. The boxes boundaries represent the 25th quantile ($q25$) and the 75th quantile ($q75$). The upper whiskers are $\min[\max(\tau), 1.5 \times (q75 - q25) + q50]$. The lower whisker has the symmetric formulation. The points are for data that are above or below the whiskers.

Figure 5 summarizes the probability distributions of ruin times and reserve for simulations for all simulations, and simulations near $\Lambda = 8$ years and $\lambda = 14$ days. Figure 5a shows that the "credit" simulations generally yield a larger median value of ruin time (between 3 and 8 years). This means that a "credit" strategy leads to a slightly longer life expectancy. The differences in the reserve are hard to see from Figure 5b, although significant with a Kolmogorov-Smirnov test (von Storch and Zwiers,
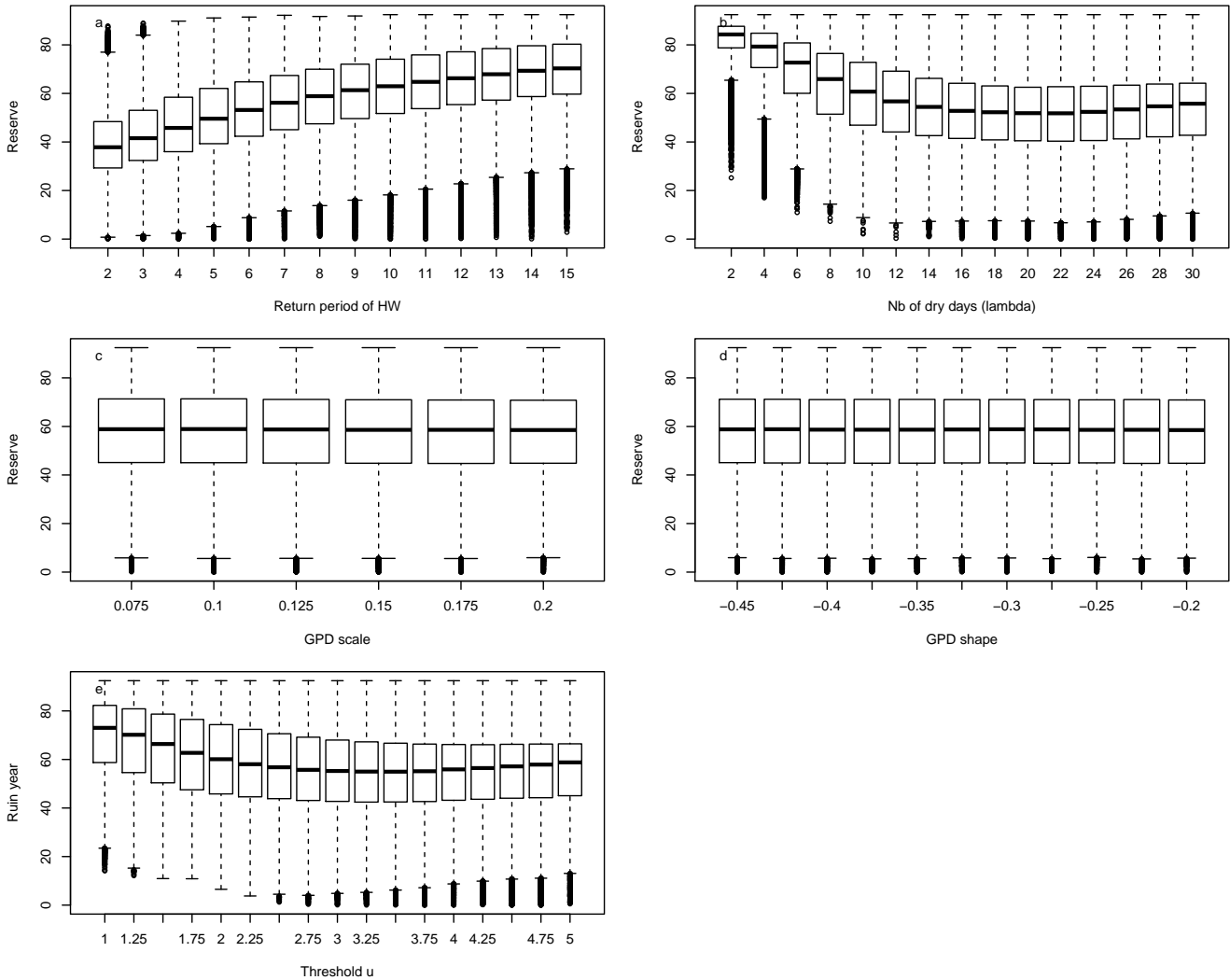
Figure 4. Dependence of probability distributions of average reserve before ruin $\langle R \rangle$ as a function of drought/heatwave (HW) return periods Λ (a), number of hot days during summers λ (b), GPD fit scale μ (c) and GPD fit shape ξ (d), and GPD threshold u (e). For each value of the control variable, a boxplot is given. The horizontal thick bar of boxplots represents the median ($q50$) of the distribution. The boxes boundaries represent the 25th quantile ($q25$) and the 75th quantile ($q75$). The upper whiskers are $\min[\max(\langle R \rangle), 1.5 \times (q75 - q25) + q50]$. The lower whisker has the symmetric formulation.

245   2001). The differences amount to ≈ 2 units of reserve, which is small compared to the optimal value. We note that "cash" ($B = 0$) simulations have a higher median reserve than the "credit" simulations for the whole ensemble or near $\Lambda = 8$ years. However, the "credit" simulations ($B = 1.5$) do have a higher median for $\lambda = 14$ days and threshold $u = 2.75$.
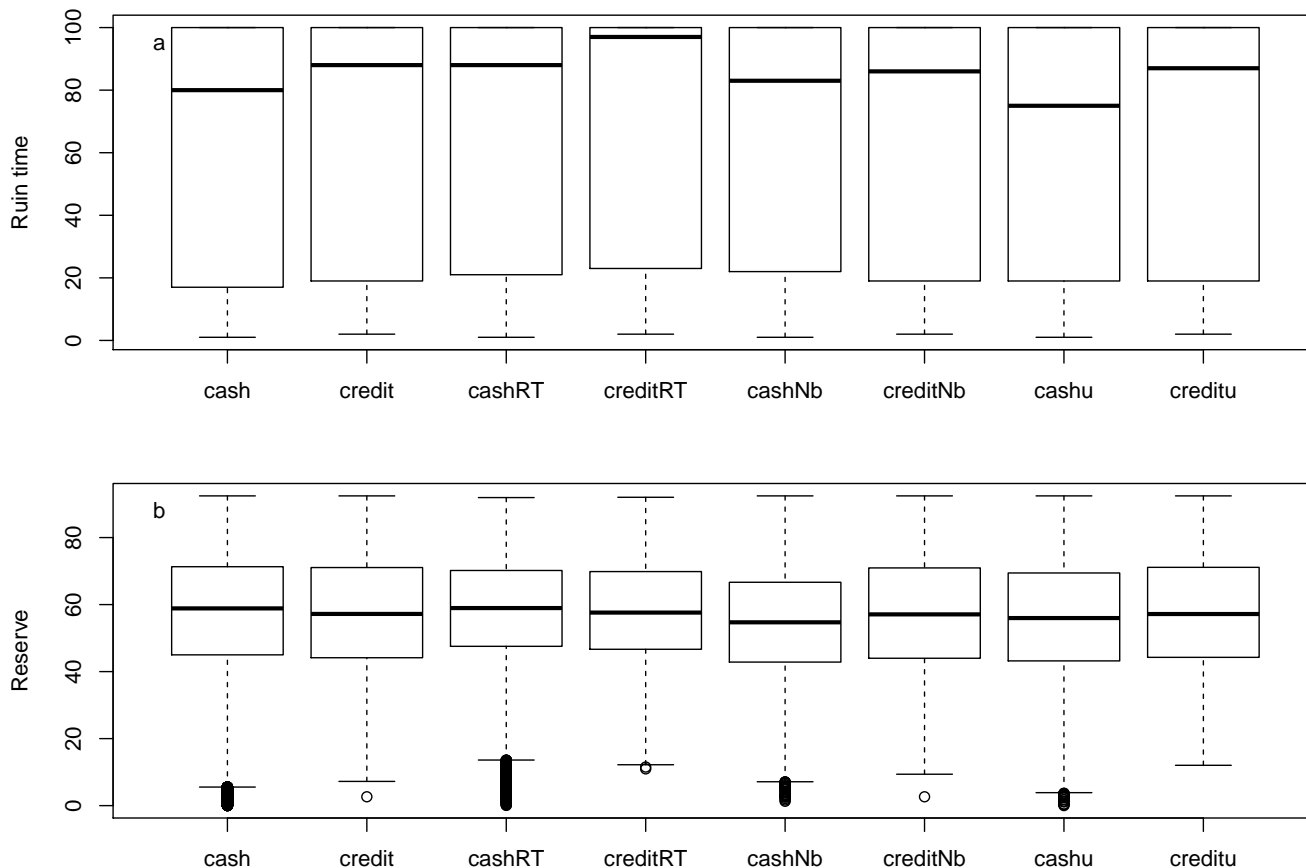
Figure 5. Conditional probability distribution of ruin times (panel a) and reserve (panel b). The first two boxplots ("cash" and "credit") are for all simulations. The "cashRT" and "creditT" boxplots are for return periods of drought/heatwaves (HW) of 8 years. The "cashNb" and "credit1Nb" boxplots are for 14 days of drought in a summer. The "cashu" and "creditu" boxplots are for a fixed threshold $u = 2.75$.

Globally, those results show the dependence of the ruin time on the coping strategy: smoothing the damages over two years increases the ruin time, for various scenarios of extremes (return time, length and intensity). However, the response of the
250 reserve depends on the parameter of extreme: a higher frequency (or lower return period Λ) favors "cash" strategies, while the intensity (linked to the duration or highest value) slightly favors "credit" strategies. Therefore, there is no binary response of this type of model to the hazard parameters, and this emphasizes the potential nonlinearity of tree response (Flach et al., 2018).

6 Conclusions

This paper presents a paradigm based on ruin theory to investigate tipping points or collapse of trees by estimating the chance

255 that systems which are subject to extreme events are damaged to the point of disappearing. It provides a quantification (and uncertainties) to the question of vulnerability of ecosystems with long expected life. This proof of concept was applied to tree growth, but it could be extended to all types of eco-systems that are vulnerable to climate hazards. This paradigm presents natural and operational features to estimate risks under climate change. It explicitly combines hazards, exposure and "fragility" to determine risks.

260 The example we took permits to make decisions on forestry from a priori information on climate change. The model we treated only accounts for one type of natural hazard. Others (including storms or fires) could be included, although the recovery rate (or "strategy") must be adapted to each type of hazard.

We have investigated how variations of the hazard parameter affect the damage function and the probability of ruin. It appears that the most critical parameters are linked to the frequency of extreme events and average intensity, which affect the

265 rate of recovery of the trees.

We have examined the impact of "strategies" to cope with extremes. Although small, this impact has a differential effect on the average tree reserve and the probability of ruin: with this model trees that have an average lower probability of ruin also have a lower average reserve, if the hazard frequency changes. If the hazard average intensity changes (longer or more intense), then trees with a lower probability of ruin also have a (slightly) higher reserve.

270 This subtlety shows the richness of this model, and emphasizes the need to have a proper definition of the hazard (Cattiaux and Ribes, 2018) and how hazards change with time, which is the topic of extreme event attribution (National Academies of Sciences Engineering and Medicine, 2016).

This study has obvious caveats. The growth/ruin model is exceedingly simple and does not reflect real trees, as the Cramer-Lundberg does not reflect the complexity of the insurance sector. The proposed tree model is mainly a proof or concept, which

275 could be enriched with other bio-physical ingredients. Nevertheless, a key point is that however complex, a ruin model should be simplifiable to a Cramer-Lundberg model.

Many mathematical papers have described the exact properties of the Cramer-Lundberg model (e.g Embrechts et al., 1997, for a review). Our tree ruin/growth model violates some of the simple assumptions of the basic Cramer-Lundberg model, namely the time independence of $R(t)$ in the "credit" mode. This forbids explicit formulas of ruin times. This is why we resort

280 to extensive numerical Monte Carlo simulations. Those simulations ($\approx 10^6$ trajectories of 100 years) take less than 4 mn on a 12 core computer, which helps circumventing this mathematical shortcoming.

The drought/heat stress indice we constructed is also rather crude and could be refined, although it was only designed to determine parameters of a Pareto distribution, and we did not use it anymore in the study because we simulate random laws (Pareto and Poisson) with parameters that are experimentally determined from the indice. All simulations were performed in

285 a stationary mode, albeit with random selections of parameters. Nonstationary simulations could be envisaged to explicitly

take climate change into account. Data from climate model simulations could hence be used to simulate hazards (e.g. Herrera-Estrada and Sheffield, 2017). This is left to future studies.

Some of the parameters (especially the impact scaling) we used were chosen heuristically. Finer in situ studies and expertise would be necessary to tune those parameters to each tree species.

290 *Code and data availability.* The simulation code and sample data to produce the drought index are available from https://zenodo.org/record/4075163

Appendix A: Drought index definition

As this paper is more a proof-of-concept for a ruin model than a detailed study (which will be performed later), we consider simplified drought/heat hazard index that can easily be computed from climatological observations. We are interested in an

295 index that reflects a compound event (Zscheischler et al., 2020) with extended dry period and high temperatures. There are a few indices of drought or aridity that consider precipitation and temperature (Baltas, 2007). The index of De Martonne (1926) normalizes cumulated precipitation and average temperature:

$$I_{DM} = \frac{P}{T+10},\tag{A1}$$

where the numerator is the cumulated precipitation and T is the mean temperature (in Celsius). This index was used to de-

300 termine drought zones. Time variations of this index can be obtained by considering only yearly or seasonal averages of precipitation and temperature. The $+10$ term in the denominator of Eq. (A1) is ad hoc to scale the respective variations of precipitation and temperature. Droughts are obtained with small values of this index (low precipitation and high temperature values).

Although easy to compute, this simple index yields a few drawbacks. The main one is that it mainly reflects wetness,

305 not drought. Most of of its variability is connected with the variability of precipitation and the upper tail of its probability distribution. Therefore seasons with little rain produce little variability in the index. One way to circumvent this would be to invert the index (i.e. consider $1/I_{DM}$). This is still not very satisfactory because the value of I_{DM} for summers with notoriously dry heatwaves (e.g., 1976 and 2003) in Europe are just within the average and do not show anything special, contrary to what is expected (Ciais et al., 2005).

310 Thus, we propose an alternative drought index, still based on daily precipitation and temperature. For a given day j, we consider D_j the frequency of precipitation: $D_j = 0$ if precipitation $P_j > 0.5$ mm/day, $D_j = 1$ if $P_j \leq 0.5$mm/day. We then construct an aridity index based on the weighted drought frequency and temperature.

$$I_{\mathrm{YV}}(t) = \sum_{j=t-30}^{t} T_j \times (D_j + a)A\exp(-(t-j)/30)\tag{A2}$$

where t is time (in days), $a \geq 0$ is a scaling constant (similar to $+10$ in Eq. (A1)) and T_j is maximum daily temperature (TX in ECA&D (Klein-Tank et al., 2002)). $A \approx 30$ is a scaling constant to ensure that the sum of exponential weights is 1. In this paper, we chose $a = 1$ after a few tuning tests to verify that the index yields high values during notoriously dry years (e.g., 1976, 2003 or 2018).

This daily index is analogous to the inverse of the De Martonne index. One refinement comes from the exponential weights that give more importance to recent days than remote days. We can then compute the monthly median, upper quantiles and maximum of I_{YV}. We compute this index by starting on March 1st, as it is generally when the tree phenology resumes after the winter season, in the Northern midlatitudes. The daily index is computed until September 30th, when the vegetative cycle is almost finished.

With this new drought index, the extreme drought/heatwaves of 1976 and 2003 do become exceptional, as expected from the literature (Ciais et al., 2005). Figure A1 compares the precipitation, temperature, de Martonne index and the new I_{YV} index for temperature and precipitation observations in Orly (near Paris, France). The precipitation or number of dry days do not yield extreme values for years with notorious heat stress in France (e.g. 1976, 2003 or 2019), as they are close to the 25–75th quantile values (Figure A1bd). Therefore, the De Martonne aridity indice does not yield particularly extreme values for those years (Figure A1c).

To better evaluate how the new index defined was a pertinent indicator for impact of climate on vegetation stress, we used the ORCHIDEE land surface model (Krinner et al., 2005) to simulate both the soil moisture and tree net primary production (NPP). We made a simulation using the ERA5 land atmospheric reanalyses at $0.1° \times 0.1°$ resolution (Hersbach et al., 2020) for the gridcell including Orly between 1981 and 2019. Atfer a spin-up of 200 years using the first 10 year of the forcing, the simulation was done for the entire period. The variations of soil moisture serve as input for the hazard function and are a refinement over precipitation only. As an indicator of vegetation damage, we consider the number of days for which NPP is below the 10th quantile (0.15 gC/day/m^2), which indicates a "risk zone" for trees (Fig. A1f).

We find a significant (negative) correlation between the percentage of dry days and relative humidity for the 1981–2019 period (Fig. A1c), with $r = -0.7$ and p-value $< 10^{-6}$. The NPP variation are significantly (anti) correlated with the I_{YV} index ($r = -0.7$, p-value $< 10^{-6}$). The percentage of days for which NPP is below the 10th quantile corresponds to the exceedances of the I_{YV} index above a high threshold (Fig. A1e). Therefore, we believe that the choice of this index carries a physical meaning and can be used as a proxy to compute the parameters of a damage function.

We computed this I_{YV} indice on five stations from ECA&D (Klein-Tank et al., 2002): Berlin, Orly, Toulouse, De Bilt and Madrid. Those five stations cover a large part western Europe.

Author contributions. PY and NV co-constructed the growth model. PY designed the ruin model simulations. NV computed the relative humidity and NPP indices for validation. PY made the figures. Both authors contributed to the text.
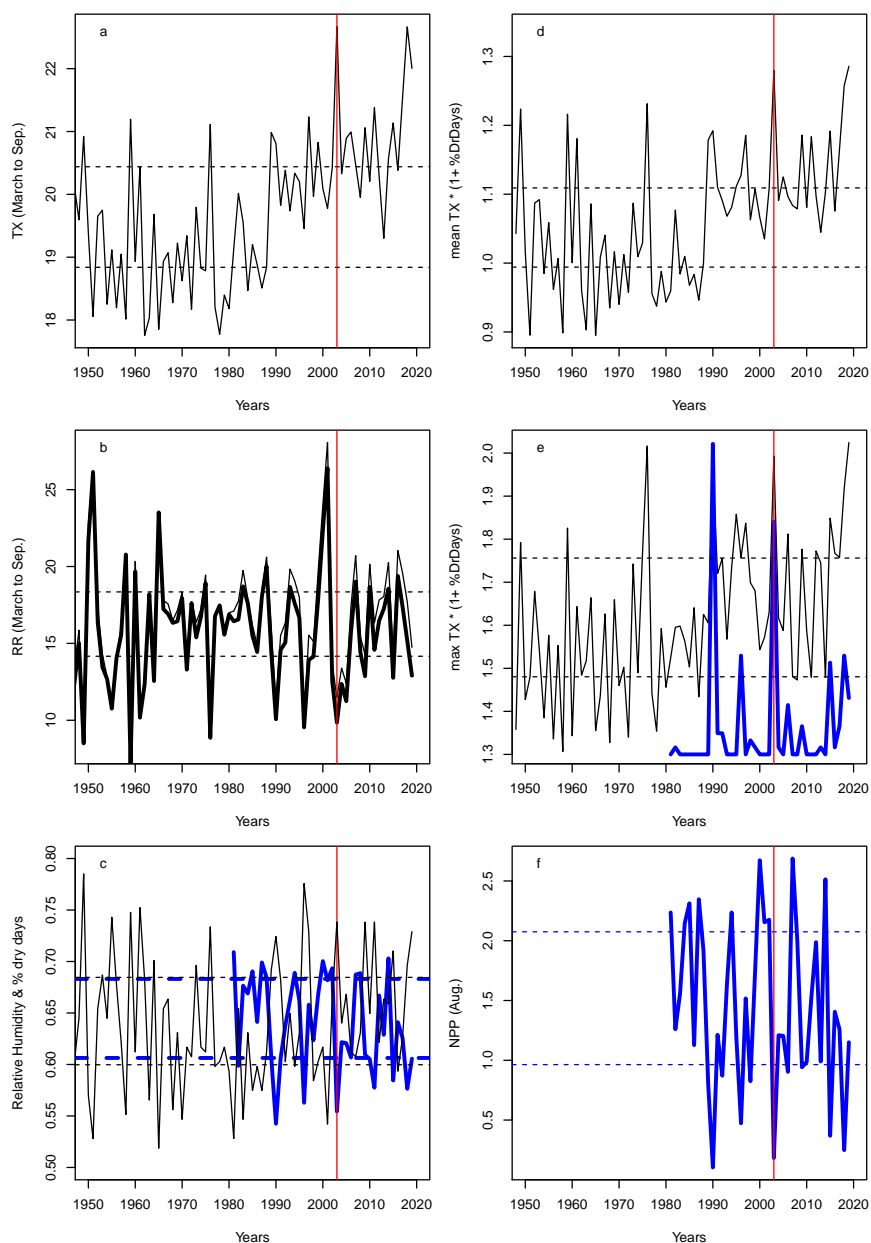
Figure A1. Variations of indices for Orly. Horizontal dashed lines for $q25$ and $q75$ quantiles. The vertical red lines are indicate 2003. a: Average (March to September) temperature in Orly. b: Average (March to September) precipitation in Orly (thin line); scaled De Martonne index (by 28) (thick black line). c: percentage of dry days between March and September (black line) and relative humidity (thick blue line). d: March to September mean of I_{YV} index. e: Daily maximum of I_{YV} index (black line) and scaled number of days when NPP is below the 10th quantile (thick blue line). f: NPP variations in Orly from an ORCHIDEE model simulation forced by the ERA5 reanalysis.

345   *Competing interests.*   The authors declare no competing interest.

Acknowledgements.   This work was supported by an ERC grant No. 338965-A2C2 and a French ANR grant (SAMPRACE).

References

Adams, H. D., Guardiola-Claramonte, M., Barron-Gafford, G. A., Villegas, J. C., Breshears, D. D., Zou, C. B., Troch, P. A., and Huxman, T. E.: Temperature sensitivity of drought-induced tree mortality portends increased regional die-off under global-change-type drought, Proceedings of the national academy of sciences, 106, 7063–7066, iSBN: 0027-8424 Publisher: National Acad Sciences, 2009.

Allen, C. D., Macalady, A. K., Chenchouni, H., Bachelet, D., McDowell, N., Vennetier, M., Kitzberger, T., Rigling, A., Breshears, D. D., and Hogg, E. T.: A global overview of drought and heat-induced tree mortality reveals emerging climate change risks for forests, Forest ecology and management, 259, 660–684, 2010.

Asmussen, S. and Albrecher, H.: Ruin probabilities, World Scientific Publishing Co Pte Ltd, 2010.

Baltas, E.: Spatial distribution of climatic indices in northern Greece, Meteorological Applications: A journal of forecasting, practical applications, training techniques and modelling, 14, 69–78, iSBN: 1350-4827 Publisher: Wiley Online Library, 2007.

Bastos, A., Ciais, P., Friedlingstein, P., Sitch, S., Pongratz, J., Fan, L., Wigneron, J. P., Weber, U., Reichstein, M., Fu, Z., Anthoni, P., Arneth, A., Haverd, V., Jain, A. K., Joetzjer, E., Knauer, J., Lienert, S., Loughran, T., McGuire, P. C., Tian, H., Viovy, N., and Zaehle, S.: Direct and seasonal legacy effects of the 2018 heat wave and drought on European ecosystem productivity, Science Advances, 6, eaba2724, https://advances.sciencemag.org/content/advances/6/24/eaba2724.full.pdf, type: 10.1126/sciadv.aba2724, 2020.

Bigler, C., Gavin, D. G., Gunning, C., and Veblen, T. T.: Drought induces lagged tree mortality in a subalpine forest in the Rocky Mountains, Oikos, 116, 1983–1994, iSBN: 0030-1299 Publisher: Wiley Online Library, 2007.

Bréda, N. and Badeau, V.: Forest tree responses to extreme drought and some biotic events: towards a selection according to hazard tolerance?, Comptes Rendus Geoscience, 340, 651–662, iSBN: 1631-0713 Publisher: Elsevier, 2008.

Cailleret, M., Jansen, S., Robert, E. M., Desoto, L., Aakala, T., Antos, J. A., Beikircher, B., Bigler, C., Bugmann, H., and Caccianiga, M.: A synthesis of radial growth patterns preceding tree mortality, Global change biology, 23, 1675–1690, iSBN: 1354-1013 Publisher: Wiley Online Library, 2017.

Cattiaux, J. and Ribes, A.: Defining single extreme weather events in a climate perspective, Bulletin of the American Meteorological Society, https://doi.org/https://doi.org/10.1175/BAMS-D-17-0281.1, 2018.

Choat, B., Jansen, S., Brodribb, T. J., Cochard, H., Delzon, S., Bhaskar, R., Bucci, S. J., Feild, T. S., Gleason, S. M., and Hacke, U. G.: Global convergence in the vulnerability of forests to drought, Nature, 491, 752, 2012.

Ciais, P., Reichstein, M., Viovy, N., Granier, A., Ogee, J., Allard, V., Aubinet, M., Buchmann, N., Bernhofer, C., Carrara, A., Chevallier, F., De Noblet, N., Friend, A., Friedlingstein, P., Grunwald, T., Heinesch, B., Keronen, P., Knohl, A., Krinner, G., Loustau, D., Manca, G., Matteucci, G., Miglietta, F., Ourcival, J., Papale, D., Pilegaard, K., Rambal, S., Seufert, G., Soussana, J., Sanz, M., Schulze, E., Vesala, T., and Valentini, R.: Europe-wide reduction in primary productivity caused by the heat and drought in 2003, Nature, 437, 529–533, <GotoISI>://000232004800045, 2005.

Coles, S.: An introduction to statistical modeling of extreme values, Springer series in statistics, Springer, London, New York, 2001.

De Martonne, E.: A new climatological function: The Aridity Index, Gauthier-Villars, Paris, France, 1926.

DeSoto, L., Cailleret, M., Sterck, F., Jansen, S., Kramer, K., Robert, E. M., Aakala, T., Amoroso, M. M., Bigler, C., and Camarero, J. J.: Low growth resilience to drought is related to future mortality risk in trees, Nature communications, 11, 1–9, iSBN: 2041-1723 Publisher: Nature Publishing Group, 2020.

Diamond, J.: Collapse: How societies choose to succeed or fail, Viking Penguin: New York, 2005.

Embrechts, P., Klüppelberg, Claudia, C., and Mikosch, T.: Modelling extremal events for insurance and finance, vol. 33 of *Applications of*
385   *mathematics*, Springer, Berlin ; New York, 1997.

Feller, W.: An Introduction to Probability Theory and Its Applications, vol. I, J. Wiley & Sons, New York, London, Sydney, 3rd edition edn.,
1950.

Flach, M., Sippel, S., Gans, F., Bastos, A., Brenning, A., Reichstein, M., and Mahecha, M. D.: Contrasting biosphere responses to hydrome-
teorological extremes: revisiting the 2010 western Russian heatwave, Biogeosciences, 16, 6067–6085, 2018.

390   Han, J. and Singh, V. P.: Forecasting of droughts and tree mortality under global warming: a review of causative mechanisms and modeling
methods, Journal of Water and Climate Change, 2020.

Haylock, M. R., Hofstra, N., Tank, A. M. G. K., Klok, E. J., Jones, P. D., and New, M.: A European daily high-resolution gridded data set
of surface temperature and precipitation for 1950-2006, J. Geophys. Res. - Atmospheres, 113, doi:10.1029/2008JD010 201, <GotoISI>:
//000260598000009, 2008.

395   Herrera-Estrada, J. E. and Sheffield, J.: Uncertainties in future projections of summer droughts and heat waves over the contiguous United
States, Journal of Climate, 30, 6225–6246, iSBN: 0894-8755, 2017.

Hersbach, H., Bell, B., Berrisford, P., Hirahara, S., Horányi, A., Muñoz-Sabater, J., Nicolas, J., Peubey, C., Radu, R., and Schepers, D.: The
ERA5 global reanalysis, Quat. J. Roy. Met. Soc., 146, 1999–2049, iSBN: 0035-9009 Publisher: Wiley Online Library, 2020.

Klein-Tank, A., Wijngaard, J., Konnen, G., Bohm, R., Demaree, G., Gocheva, A., Mileta, M., Pashiardis, S., Hejkrlik, L., Kern-Hansen,
400   C., Heino, R., Bessemoulin, P., Muller-Westermeier, G., Tzanakou, M., Szalai, S., Palsdottir, T., Fitzgerald, D., Rubin, S., Capaldo, M.,
Maugeri, M., Leitass, A., Bukantis, A., Aberfeld, R., Van Engelen, A., Forland, E., Mietus, M., Coelho, F., Mares, C., Razuvaev, V.,
Nieplova, E., Cegnar, T., Lopez, J., Dahlstrom, B., Moberg, A., Kirchhofer, W., Ceylan, A., Pachaliuk, O., Alexander, L., and Petrovic, P.:
Daily dataset of 20th-century surface air temperature and precipitation series for the European Climate Assessment, Int. J. Climatol., 22,
1441–1453, 2002.

405   Krinner, G., Viovy, N., de Noblet-Ducoudré, N., Ogée, J., Polcher, J., Friedlingstein, P., Ciais, P., Sitch, S., and Prentice, I. C.:
A dynamic global vegetation model for studies of the coupled atmosphere-biosphere system, Global Biogeochemical Cycles, 19,
https://doi.org/10.1029/2003GB002199, iSBN: 0886-6236 Publisher: Wiley Online Library, 2005.

Lenton, T. M., Held, H., Kriegler, E., Hall, J. W., Lucht, W., Rahmstorf, S., and Schellnhuber, H. J.: Tipping elements in the Earth's climate
system, Proc. Natl. Acad. Sci. USA, 105, 1786–1793, https://doi.org/DOI 10.1073/pnas.0705414105, <GotoISI>://000253261900005,
410   2008.

Levermann, A., Bamber, J. L., Drijfhout, S., Ganopolski, A., Haeberli, W., Harris, N. R. P., Huss, M., Kruger, K., Lenton, T. M., Lindsay,
R. W., Notz, D., Wadhams, P., and Weber, S.: Potential climatic transitions with profound impact on Europe Review of the current
state of six 'tipping elements of the climate system', Climatic Change, 110, 845–878, https://doi.org/DOI 10.1007/s10584-011-0126-5,
<GotoISI>://000299346900019, 2012.

415   Lundberg, F.: Approximerad framstallning af sannolikhetsfunktionen: Aterforsakring af kollektivrisker, Almqvist & Wiksell, 1903.

Matusick, G., Ruthrof, K. X., Kala, J., Brouwers, N. C., Breshears, D. D., and Hardy, G. E. S. J.: Chronic historical drought legacy exacerbates
tree mortality and crown dieback during acute heatwave-compounded drought, Environmental Research Letters, 13, 095 002, iSBN: 1748-
9326 Publisher: IOP Publishing, 2018.

Mitchell, P. J., O'Grady, A. P., Tissue, D. T., White, D. A., Ottenschlaeger, M. L., and Pinkard, E. A.: Drought response strategies define the
420   relative contributions of hydraulic dysfunction and carbohydrate depletion during tree mortality, New Phytologist, 197, 862–872, iSBN:
0028-646X Publisher: Wiley Online Library, 2013.

National Academies of Sciences Engineering and Medicine, ed.: Attribution of Extreme Weather Events in the Context of Climate Change, The National Academies Press, Washington, DC, https://doi.org/10.17226/21852, www.nap.edu/catalog/21852/attribution-of-extreme-weather-events-in-the-context-of-climate-change, 2016.

425 Sippel, S., Reichstein, M., Ma, X., Mahecha, M. D., Lange, H., Flach, M., and Frank, D.: Drought, heat, and the carbon cycle: A review, Current Climate Change Reports, 4, 266–286, 2018.

Teuling, A. J., Seneviratne, S. I., Stöckli, R., Reichstein, M., Moors, E., Ciais, P., Luyssaert, S., Van Den Hurk, B., Ammann, C., and Bernhofer, C.: Contrasting response of European forest and grassland energy exchange to heatwaves, Nature Geoscience, 3, 722–727, iSBN: 1752-0908 Publisher: Nature Publishing Group, 2010.

430 van der Molen, M. K., Dolman, A. J., Ciais, P., Eglin, T., Gobron, N., Law, B. E., Meir, P., Peters, W., Phillips, O. L., and Reichstein, M.: Drought and ecosystem carbon cycling, Agricultural and Forest Meteorology, 151, 765–773, iSBN: 0168-1923 Publisher: Elsevier, 2011.

Villalba, R. and Veblen, T. T.: Influences of large-scale climatic variability on episodic tree mortality in northern Patagonia, Ecology, 79, 2624–2640, iSBN: 1939-9170 Publisher: Wiley Online Library, 1998.

Villalba, R., Cook, E., Jacoby, G., D'Arrigo, R., Veblen, T., and Jones, P.: Tree-ring based reconstructions of northern Patagonia precipitation 435 since AD 1600, HOLOCENE, 8, 659–674, <GotoISI>://000077236500002, 1998.

von Buttlar, J., Zscheischler, J., Rammig, A., Sippel, S., Reichstein, M., Knohl, A., Jung, M., Menzer, O., Arain, M. A., and Buchmann, N.: Impacts of droughts and extreme temperature events on gross primary production and ecosystem respiration: A systematic assessment across ecosystems and climate zones, Biogeosciences Discussions, iSBN: 1810-6277 Publisher: Copernicus, 2017.

von Storch, H. and Zwiers, F. W.: Statistical Analysis in Climate Research, Cambridge University Press, Cambridge, 2001.

440 Wigneron, J.-P., Fan, L., Ciais, P., Bastos, A., Brandt, M., Chave, J., Saatchi, S., Baccini, A., and Fensholt, R.: Tropical forests did not recover from the strong 2015–2016 El Niño event, Science advances, 6, eaay4603, iSBN: 2375-2548 Publisher: American Association for the Advancement of Science, 2020.

Zscheischler, J., Martius, O., Westra, S., Bevacqua, E., Raymond, C., Horton, R. M., van den Hurk, B., AghaKouchak, A., Jézéquel, A., and Mahecha, M. D.: A typology of compound weather and climate events, Nature reviews earth & environment, pp. 1–15, iSBN: 2662-138X 445 Publisher: Nature Publishing Group, 2020.